Characteristics and processing of aqueous secondary organic aerosols during autumn in suburban Eastern China: role of aerosol liquid water, aerosol acidity, and photochemistry

Qiu Wang[1], Tengyu Liu[1,2,3*], Weiqi Xu[4], Jinbo Wang[1,5], Dafeng Ge[1], Caijun Zhu[1], Chuanhua Ren[1], Jiaping Wang[1,2], Qiaozhi Zha[1,2], Ximeng Qi[1,2], Wei Nie[1,2], Xuguang Chi[1,2], Sijia Lou[1,2,3], Xin Huang[1,2,3], Aijun Ding[1,2,3]

[1]School of Atmospheric Sciences, Nanjing University, Nanjing, 210023, China

[2]National Observation and Research Station for Atmospheric Processes and Environmental Change in Yangtze River Delta, Nanjing, 210023, China

[3]Frontiers Science Center for Critical Earth Material Cycling, Nanjing University, Nanjing, 210023, China

[4]State Key Laboratory of Atmospheric Environment and Extreme Meteorology, Institute of Atmospheric Physics, Chinese Academy of Sciences, Beijing 100029, China

[5]Now at National Satellite Meteorological Center, China Meteorological Administration, Beijing 100081, China

[*]Corresponding author: Tengyu Liu (tengyu.liu@nju.edu.cn)

Abstract

Aqueous-phase secondary organic aerosols (aqSOA) constitute a large fraction of SOA, thereby exerting significant influence on air quality, climate, and human health. However, its formation pathways under real ambient conditions in Chinese urban regions remain insufficiently constrained. We conducted field measurements of particulate matters (PM) composition by deploying high-resolution aerosol mass spectrometry in a suburban environment during autumn in Nanjing, China. The characteristics and formation pathways of aqSOA are comprehensively investigated by using Positive Matrix Factorization (PMF) method. Our results show that aqSOA accounted for 27.6% of oxidized organic aerosols, exhibiting elevated O:C ratios (0.78) and strong correlations with nitrate and aerosol liquid water (ALW). The important role of acid-catalyzed reactions is also revealed by the enhanced production of aqSOA at lower aerosol pH conditions. Under elevated nitrate and ALW levels, a pronounced morning aqSOA peak was frequently observed; whereas a noon-time aqSOA peak was also observed on several days, likely governed by photochemistry and aqueous-phase reactions. These findings highlight the critical roles of nitrate, ALW, acidity, and photochemistry in driving aqSOA production in polluted urban environments. This study advances the mechanistic understanding of aqSOA formation and provides insights into the mitigation of SOA in the Eastern China.

1 Introduction

Organic aerosols (OA) significantly affect air quality, human health, and climate by influencing radiative forcing and cloud formation (Kanakidou et al., 2005; Zhou et al., 2019). Secondary organic aerosols (SOA) can contribute 30–70% of total organic aerosols (Huang et al., 2014; Xian et al., 2023). The formation of SOA has been attributed mainly to gas-phase oxidation of volatile organic compounds (VOCs), where the oxidized products subsequently partition into the aerosol phase (Hennigan et al., 2009; Seinfeld and Pankow, 2003; Ziemann and Atkinson, 2012). Recently, growing evidence highlights the important role of SOA generated through aqueous-phase processes in cloud droplets, fog, and aerosol liquid water (ALW) (Ervens et al., 2011; Kim et al., 2019; Sun et al., 2010). However, the formation mechanisms and sources of aqueous-phase SOA (aqSOA) in Chinese urban regions remain highly uncertain (Ervens et al., 2011; Huang et al., 2025; McNeill, 2015) .

In recent years, concentrations of OA have gradually declined across many regions in China due to the implementation of air pollution control measures, but the relative contribution of SOA has increased markedly (Chen et al., 2024; Huang et al., 2025), with aqSOA constituting a substantial fraction. Numerous studies have demonstrated that elevated ALW can significantly promote aqSOA formation during winter haze episodes through multiphase reactions (Chen et al., 2021; Feng et al., 2022; Liu et al., 2019; Peng et al., 2021; Sun et al., 2016, 2019; Wang et al., 2023; Xiao et al., 2022; Xu et al., 2017; Zhao et al., 2019). Still, the exact processes driving aqSOA formation is not fully characterized. Field observations in urban Beijing have shown that ring-

59 breaking oxidation and functionalization of polycyclic aromatic hydrocarbons of fossil-
60 fuel-derived primary organic aerosols could lead to rapid aqSOA formation at high
61 relative humidity (RH) during winter haze episodes (Wang et al., 2021). Another field
62 study conducted in the North China Plain showed that the formation of aqSOA could
63 be largely enhanced under favorable photochemical conditions with precursors
64 originated from biomass burning activities (Kuang et al., 2020). Recently, field
65 measurements in Hebei reported that high nitrate may support the potential
66 formation/transformation from POA-related components to aqSOA (Gu et al., 2023).
67 Laboratory studies reveal that accretion reactions, which play a crucial role in SOA
68 formation, are highly sensitive to pH levels (Tilgner et al., 2021). Moreover, under the
69 emerging dominance of nitrate in aerosol composition (Huang et al., 2025), the
70 interplay among nitrate, ALW, and pH may complex the aqSOA formation and requires
71 further investigation.

72 The Yangtze River Delta (YRD) region is one of the most densely populated and
73 economically developed areas in China, characterized by intensive industrial activity,
74 heavy traffic emissions, frequent regional pollution episodes, and high relative
75 humidity (Liu et al., 2025). Several previous studies have examined aqSOA processes
76 in this region (Wang et al., 2016; Wu et al., 2018; Xian et al., 2023), but uncertainties
77 regarding its sources, controlling factors, and formation mechanisms still remained.
78 Consequently, it is challenging for current models to precisely simulate aqSOA and its
79 contribution to the YRD region (Ervens et al., 2011; Rogers et al., 2025).

80 In this study, we conducted real-time measurements of OA at the National

Observation and Research Station for Atmospheric Processes and Environmental Change in Yangtze River Delta (SORPES) located in suburban Nanjing in the western YRD region during the autumn of 2020. The chemical characteristics and formation mechanisms of aqSOA, as well as the roles of nitrate, ALW, and aerosol acidity) are investigated. By classifying diurnal variation patterns of aqSOA, we assessed the relative roles of photochemical and aqueous-phase processes. The results provide new insights into regional aqSOA formation in the YRD and have implications for the development of effective air pollution control strategies.

2 Materials and Methods

2.1 Sampling Site

The field campaign was conducted from 13 October to 30 December in 2020 at SORPES station (118°57′E, 32°07′N) located in the Xianlin campus of Nanjing University in Nanjing, China. This is a representative station of western YRD, surrounded by high vegetation cover, and also subject to abundant anthropogenic emissions (Ding et al., 2016, 2019; Dou et al., 2025; Liu et al., 2025).

2.2 Instrumentation

Real-time non-refractory PM_1 composition was measured using a high-resolution time-of-flight aerosol mass spectrometer (HR-ToF-AMS; hereafter, AMS; Aerodyne Research Inc.). An aerodynamic PM_1 lens was used to focus the particle into a beam, which was then impacted on the heated tungsten surface (~600°C) and flash-vaporized. In our study, ambient aerosols were passed through a ~2 m long stainless-steel sampling tube, dried by a Nafion drying tube, and then introduced into the AMS. In order to

obtain highly sensitive data, AMS was operated in V mode with a time resolution of 2 minutes (DeCarlo et al., 2006).

Other instruments were also employed at SORPES in support of these measurements. Black carbon (BC) was measured by the photoacoustic extinctiometer (PAX, Droplet Measurement Technologies Inc., USA). The meteorological parameters and gaseous pollutants were also measured simultaneously. Ozone (O_3), carbon monoxide (CO), nitric oxide (NO), nitrogen oxides (NO_x) and sulfur dioxide (SO_2) were measured using online analyzers (Thermo Fisher Scientific, USA). Ammonia (NH_3) was measured by the Picarro G2103 gas analyzer (Picarro Inc., USA) (Liu et al., 2024). Temperature, RH and other meteorological parameters were monitored by meteorological sensors (GRWS100, Campbell, USA).

2.3 Data Analysis

The AMS data were processed by SQUIRREL (version 1.60P) and PIKA (version 1.20P) from the ToF-AMS Software Downloads Web page (http://cires.colorado.edu/jimenez-group/ToFAMSResources/ToFSoftware/index.html). The ionization efficiency (IE) was calibrated using 300 nm pure ammonium nitrate before and after the campaign. The relative ionization efficiency (RIE) of ammonium was determined from pure ammonium nitrate, yielding a value of 3.52. RIE values for OA, nitrate, sulfate, and chloride were set to their default values of 1.4, 1.1, 1.2, and 1.3, respectively (Canagaratna et al., 2007). As well, the collection efficiency (CE) was assigned a typical value of 0.5 for common environments, although it is recognized that this constant value may introduce additional uncertainty during periods with high nitrate content. Element

ratios, including H: C, O: C, N: C and OM: OC, are calculated using the Improved-Ambient method (Canagaratna et al., 2015).

In addition, ALW content and aerosol acidity that are associated with inorganic species were estimated by the Extended Aerosol Inorganics Model (E-AIM), which is a well-known inorganic thermodynamic model without simplifying assumptions (Clegg et al. 1998; Wexler and Clegg 2002; Pye et al. 2020). The key inputs to the E-AIM model include temperature, relative humidity, and the concentrations of inorganic ions (sulfate, nitrate, ammonium, chloride) as well as gas-phase ammonia. The main sources of uncertainty stem from thermodynamic parameters and the uncertainties of measured inorganic ions. In this study, the ALW associated with the hygroscopicity of organics was estimated following the method of Nguyen et al. (2016) using the κ-Kohler theory and the Zdanovskii−Stokes−Robinson mixing rule. The estimated organic-associated ALW was only 10.7% of that associated with the inorganic aerosols. Therefore, the organic-associated ALW was neglected in the subsequent analysis.

2.4 Source Apportionment of OA

Positive Matrix Factorization (PMF) analysis was applied to the high-resolution mass spectra of organic matrix for m/z 12 – 120 to resolve distinct OA factors from specific sources (Paatero and Tapper, 1994; Ulbrich et al., 2009). The data and error matrices were treated according to the procedures detailed in DeCarlo et al. (2010). By comparing the mass spectral profiles with previous studies and correlations with time series of tracers, five OA factors with fpeak = 0 were selected, including one primary organic aerosol (POA) factor, one nitrogenous OA (NOA) factor, and three SOA factors,

namely, less-oxidized oxygenated OA (LO-OOA), more-oxidized OOA (MO-OOA), and aqSOA. The detailed diagnostic plots are shown in Figures S1 and S2 in the supporting information.

AqSOA exhibited strong correlations with unique fragment ions that are widely recognized as markers of aqueous-phase secondary products (Sun et al., 2016; Xu et al., 2019). For instance, significant correlations were observed with $C_2O_2^+$ (m/z 56, r = 0.77), a typical fragment of oxalate-related species, and with CH_3SO^+ (m/z 63, r = 0.90), which is indicative of organosulfur compounds (Figure S3). These results provide chemical evidence supporting the aqueous-phase origin of aqSOA in Nanjing. Among these five OA factors, aqSOA exhibits typical characteristics of highly oxidized organic aerosols: fraction of m/z 44 (CO_2^+, primarily from carboxylic acids and highly oxidized compounds) (Heald et al., 2010) in total signals exceeded that of m/z 43 (typically representing less oxidized compounds) (Figure S2). Elemental analysis further indicated a strongly oxygenated character, with an average H:C ratio of 1.80 and an O:C ratio of 0.78. These values are comparable to those reported in other regions, such as northern Italy and Beijing (Gilardoni et al., 2016; Xu et al., 2019). The N:C ratio (0.05) was also elevated and similar to wintertime values observed in Beijing (N:C = 0.045; Xu et al. 2017), suggesting nitrogen-containing compound formation via aqueous-phase processing.

3.Results and Discussions

3.1 General Characteristics of aqSOA

The meteorological conditions in Nanjing were overall stable during the field campaign

(October-December), with an average temperature and RH of 14.6 ± 4.6 °C and 65.1 ± 17.9%, respectively (Figure S6). The diurnal variation of RH ranged from 50% to 85%, resulting in relatively humid air conditions that favored aqueous-phase chemical reactions. The average wind speed of the prevailing northerly wind was relatively low (0.21 ± 0.16 m/s), resulting in the accumulation of local pollutants. In particular, the average NR-PM_1 concentration was 37.3 ± 20.6 μg/m³, indicating frequently occurred particulate matter pollution during this period.

Analysis of aerosol chemical composition revealed that organic aerosol was the dominant NR-PM_1 component in Nanjing, accounting for 40.9% of the total PM_1 concentration, evidently higher than nitrate (30.7%) and sulfate (13.9%; Figure S6). The time series of aqSOA showed significant variation, with peak concentrations up to 15.7 μg/m³ (Figure 1a). The average concentration of aqSOA during the campaign was 3.1 μg/m³, accounting for 20.2% (62.7% in maximum) of the total OA and 27.6% (78.2% in maximum) of the total SOA (Figure 1b). The average fraction of aqSOA in OA was much higher than Beijing (13-17%) (Zhao et al., 2019), indicating an important role of aqueous-phase processes in SOA formation in Nanjing. Moreover, both aqSOA concentrations and their relative contribution to total organic aerosol increased significantly with increasing RH (Figure S7a), which was likely due to the increased availability of the aqueous reaction medium enhanced by water uptake by aerosols, which is crucial for the aqSOA formation. This is further confirmed with the sharply increased contribution of aqSOA to OA (up to 62.7%) at RH levels above 80%, suggesting that high-humidity environments in suburban Nanjing substantially

promoted aqSOA formation through enhanced aqueous-phase chemistry.

The Van Krevelen diagram (Heald et al., 2010) provided further insights into the chemical aging of OA (Figure S8). The H:C vs. O:C slope was near -0.5, indicating OA oxidation primarily involving carboxylic acid and peroxide or alcohol functional groups addition without fragmentation and/or the addition of carboxylic acid functional groups with fragmentation (Ng et al., 2011). In particular, OA observed under high RH conditions (>80%) clustered in the upper plot region, suggesting distinct chemical evolution of OA when aqueous-phase reactions were involved. Specifically, the nearly zero slope of the relationship among POA, LO-OOA and aqSOA suggests that the observed increase in the O:C ratio of aqSOA may be related to oligomerization and hydroxyl formation through dark chemistry processes (Lim et al., 2010).

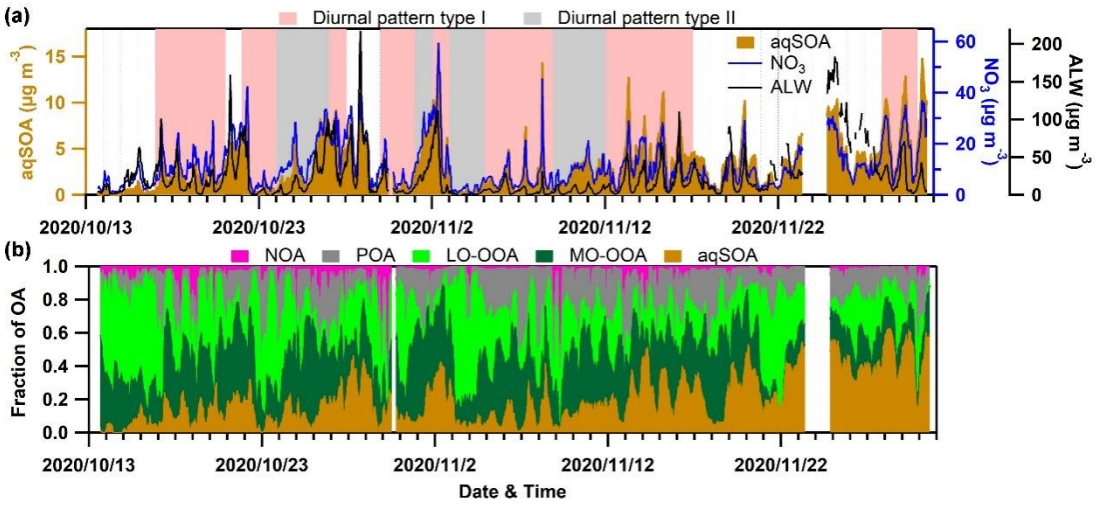

Figure 1. (a) Time series of aqSOA and nitrate concentrations. The pink area represents diurnal pattern type I, while the grey area represents diurnal pattern type II. (b) Time series of the fraction of five OA factors.

3.2 Enhanced aqSOA Formation Driven by Nitrate, ALW, and Acid Catalysis

As a strongly hygroscopic component, nitrate aerosol can enhance aerosol water uptake, thereby modifying the aqueous microenvironment for SOA production (Hodas et al., 2014; Sullivan et al., 2016). We observed strong correlation between aqSOA and nitrate concentrations (R^2 = 0.83; Figure 2a) during the observation period, and the variation of aqSOA was highly consistent with that of nitrate aerosol (Figure 1a). This suggests that nitrate aerosols may contribute importantly to aqSOA formation in Nanjing, potentially mediated by their influence on ALW and/or aqueous reactions. We estimated that the average contribution of organic nitrates to the total nitrate was approximately 9.5% by assuming a NO^+ to NO_2^+ ratio of 10 for organic nitrates (Farmer et al., 2010). Thus, organic nitrates can be considered negligible in this study.

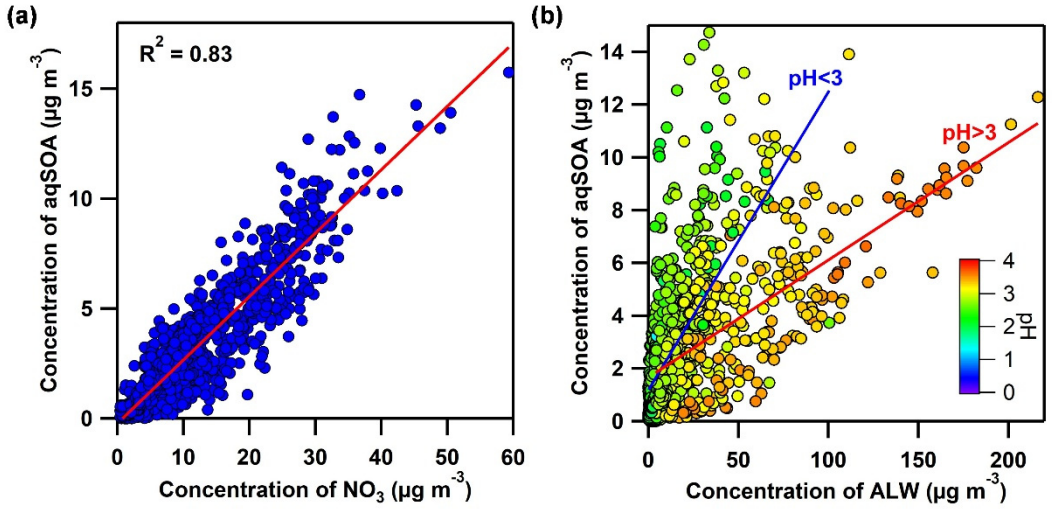

Figure 2. (a) Scatter plot of aqSOA and nitrate concentrations. (b) Scatter plot of aqSOA and ALW concentrations, colored by aerosol pH. The blue line represents the fitted line for data with aerosol pH < 3, while the red line represents the fitted line for

224 data with aerosol pH > 3.

225

226 The correlation between aqSOA and aerosol liquid water (ALW; r = 0.63; Figure
227 2b), which is mainly derived from the hygroscopic growth of inorganic salts such as
228 nitrate, was moderate compared to nitrate. Still, their positive relationship indicates that
229 higher ALW levels may enhance aqueous-phase chemical processes by providing the
230 medium in which multiphase reactions can occur (Hodas et al., 2014). The presence of
231 ALW promotes the partitioning of water-soluble organic precursors and allows for
232 subsequent aqueous-phase reactions contributing to aqSOA formation. The results are
233 consistent with previous studies in humid urban environments (Chen et al., 2021; Duan
234 et al., 2022; Kuang et al., 2020).

235 In addition to ALW, aerosol acidity also exerted a strong influence on aqSOA
236 yields during the campaign (Lim et al., 2010; Tilgner et al., 2021). To illustrate, the
237 dataset was separated by aerosol pH (pH < 3 vs. pH > 3) (Figure 2b), the slopes of
238 ALW-aqSOA correlations decreased with increasing pH, indicating that aqSOA
239 production was higher under more acidic conditions at the same ALW level. This
240 pattern demonstrates the importance of acid-catalyzed reactions in driving aqSOA
241 formation. Previous studies have demonstrated that under acidic conditions (low pH,
242 high H^+ concentration), non-oxidative aqueous organic chemical processes, such as
243 accretion reactions (aldol condensation, hemiacetal and acetal formation, and the
244 esterification of carboxylic acids) are important formation pathways of aqSOA
245 (Freedman et al., 2019; Tilgner et al., 2021). For example, the hydration of

methylglyoxal and its subsequent acetal formation are highly pH-dependent, requiring a pH of less than 3.5 to occur (Yasmeen et al., 2010). As aerosol pH increases (lower H^+ availability), the catalytic efficiency of these acid-driven reactions diminishes, leading to a reduction in aqSOA production efficiency Collectively, these findings suggest that aerosol acidity plays a pivotal regulatory role in aqSOA formation, linking aqueous chemistry to the broader context of aerosol physicochemical properties in Nanjing.

Thus, our measurements revealed a synergistic interplay among nitrate, ALW, and aerosol acidity in regulating aqSOA formation in Nanjing. Nitrate enhances the ALW content, which in turn promotes aqueous-phase reactions, while aerosol acidity governs the efficiency of these chemical processes. These processes together constituted the formation mechanism of aqSOA during the observation period.

3.3 Synergistic Role of Aqueous and Photochemical Processes

During the campaign, the average diurnal variation of aqSOA in Nanjing exhibited a distinct morning peak at approximately 09:00 local time (Figure S2d). This pattern is different from most of the previous urban observations, where aqSOA concentrations typically peak during nighttime periods (Sun et al., 2016; Xu et al., 2019; Gu et al., 2023). To address this, the time series of aqSOA was analyzed on a daily basis, with rainy days excluded. Based on this analysis, two distinct diurnal variation patterns were identified: type I (22 days) and type II (9 days) (Figure 1a). For diurnal pattern type I, the daily variation of aqSOA exhibits a pronounced morning peak, whereas the daytime concentration of aqSOA shows a noon peak for diurnal pattern type II (Figure 3). These

two distinct diurnal patterns of aqSOA could be attributed to multiple formation mechanisms of aqSOA or different meteorological conditions. It should be noted that the observed morning peak around 09:00–10:00 may be modulated not only by chemical production but also by concurrent physical processes, such as morning boundary-layer evolution and mixing/dilution effects. Nevertheless, the diurnal patterns and classification discussed herein are interpreted primarily under chemically constrained conditions, and the main conclusions about aqSOA formation pathways rely chiefly on chemical relationships and correlations.

During diurnal pattern type I, aqSOA concentrations exhibited a pronounced single peak between 09:00 and 10:00 local time, following a period of continuous nighttime accumulation from approximately 20:00 to 07:00 (Figure 3a). Notably, the aqSOA peak lagged behind the nitrate peak by about one hour (based on the average peak-time difference), and nocturnal increases in nitrate, ALW, and aqSOA were highly synchronized. This ~1 h lag may be attributed to the kinetic limitations of the nitrate-mediated aqSOA formation processes. Compared with type II, nighttime meteorological conditions during type I were characterized by higher RH (73.1% vs. 61.2%) and ALW concentrations (34.2 μg/m³ vs. 12.6 μg/m³). Such humid conditions favor the formation of both nitrate and ALW, thereby enhancing aqSOA production through aqueous-phase reactions. Moreover, the higher RH conditions observed during type I events could further promote aqueous reaction pathways, as the nitrate formation from N_2O_5 hydrolysis on aqueous aerosol surfaces is strongly facilitated under such conditions (Sun et al., 2018). Overall, these observations indicate that aqSOA

production under type I conditions is predominantly controlled by aerosol aqueous-phase processes, highlighting the important role of nocturnal multiphase chemistry in driving morning aqSOA peaks.

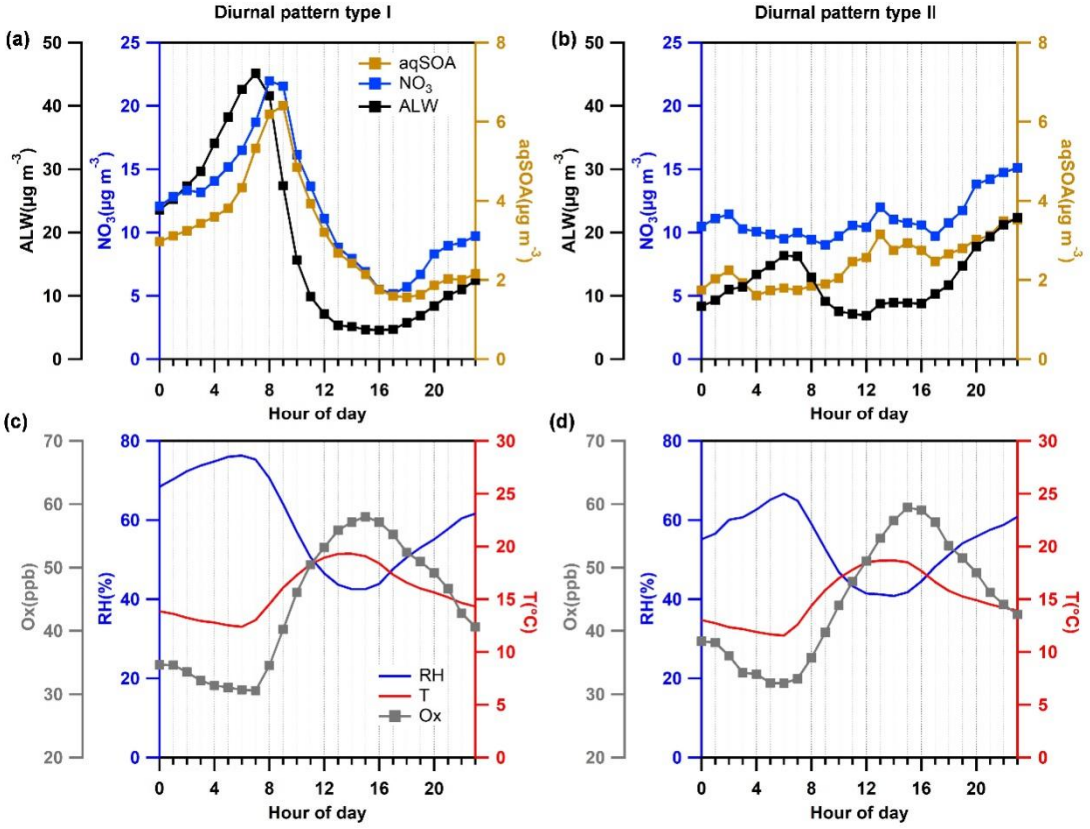

Figure 3. Diurnal variations for SOA, ALW, and nitrate in diurnal pattern types I (a) and II (b). Diurnal variations for temperature, humidity, and O_x concentration in diurnal pattern types I (c) and II (d).

In contrast, aqSOA concentrations gradually increased during the daytime and peaked around 13:00 local time (Figure 3b) during diurnal pattern type II, indicating an influence of photochemical processes. The diurnal variation of aqSOA is consistent with that of nitrate aerosols. This suggests that enhanced photochemical activity is

303 associated with nitrate aerosol formation, which may subsequently mediate aqSOA
304 production via water uptake. O_x is commonly regarded as a tracer for photochemical
305 processes. The relationship between daytime (08:00–17:00) aqSOA concentrations and
306 O_x levels was examined for both diurnal patterns (Figure 4). For diurnal type I, no
307 significant correlation was observed, suggesting that daytime photochemistry played a
308 minimal role in aqSOA production under these conditions. In contrast, diurnal type II
309 displayed a positive correlation, implying that aqSOA formation was partially related
310 to the photochemical processes.
311

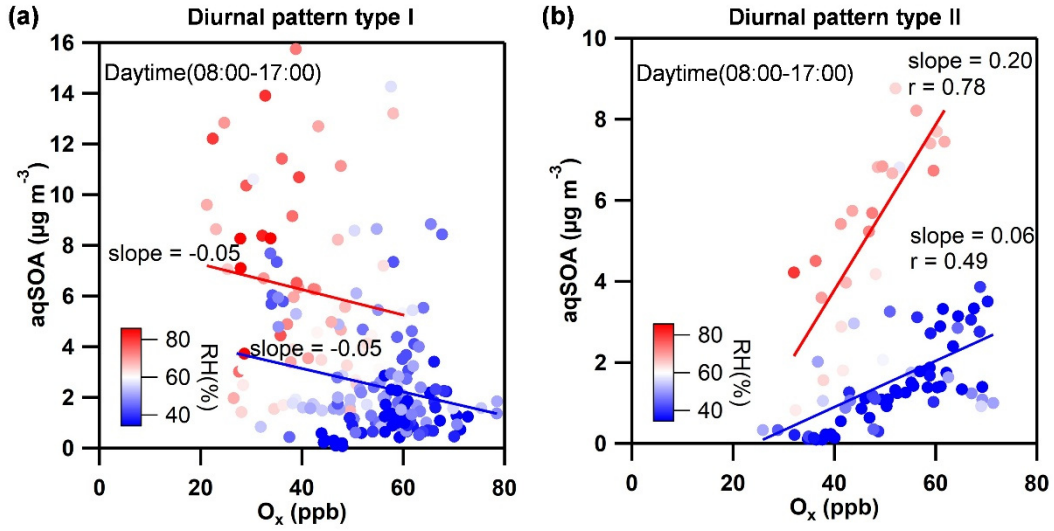

312

313 **Figure 4**. Scatter plots of aqSOA and O_x for Diurnal pattern types I (a) and II (b). Data
314 points are colored by RH, with red and blue lines representing fits for RH > 60% and
315 RH < 60% respectively. For diurnal pattern type I, the correlation coefficient was -0.22
316 (N = 151, $p < 0.01$) during daytime with RH < 60%, and r = -0.14 (N = 59, $p = 0.3$)
317 when RH > 60%. For diurnal pattern type II, the correlation coefficient was 0.49 (N =
318 67, $p < 0.01$) under RH < 60%, and r = 0.78 (N = 23, $p < 0.01$) under RH > 60%.

Further analysis revealed that the slope of the aqSOA-O_x relationship under high RH conditions in diurnal type II was approximately three times higher than that under low RH conditions. This is because higher RH likely enhanced the partitioning of semi-volatile photochemical oxidation products into the aqueous phase and promoted aqueous-phase photochemical reactions, thereby facilitating aqSOA formation. These results indicate that daytime aqSOA production during type II is governed by the combined effects of photochemical oxidation and humidity-dependent aqueous processing.

4. Conclusions

We analyzed the characteristics and formation mechanisms of aqSOA in the autumn season in Nanjing, where aqSOA was found to constitute a significant fraction of organic aerosols (20.2%). The results demonstrate that nitrate, ALW, and aerosol acidity act in concert to regulate aqSOA formation, with nitrate serving as a critical driver through its strong hygroscopicity. We observed the occurrence of a distinct morning peak of aqSOA in the YRD region, a feature that differs from most of the previously reported studies in urban environments. Based on diurnal variation analysis, two distinct diurnal patterns were identified: type I, dominated by nighttime aqueous-phase chemistry linked to nitrate and ALW accumulation; and Type II, shaped primarily by daytime photochemical oxidation. These findings highlight that aqSOA formation in this megacity is governed by the synergistic effects of both nocturnal aqueous

reactions and daytime photochemical processes.

China is strictly controlling SO_2 emissions, which has led to a decrease in sulfate content in atmospheric particulate matter. Nitrate is becoming a more important inorganic component of $PM_{2.5}$, and its role in promoting aqSOA formation will become even more significant. Although this study did not directly resolve the specific precursor compounds of aqSOA, our results still highlight the importance of paying greater attention to nitrate-driven aqueous processes in future air quality assessments. In particular, coordinated management of nitrogen oxides (NO_x) alongside traditional particulate matter controls may provide an effective pathway for mitigating aqSOA burdens in a post-sulfate-dominated atmosphere.

Author contributions

T.L. and A.D. designed the research project; J.W., D.G., C.Z., C.R., W.X., J.W., W.N., X.C., S.L. and X.H. performed the research; Q.W., Q.Z., and X.Q. analyzed data; Q.W., Q.Z., and T.L. wrote the paper. All authors participated in the relevant scientific discussion and commented on the manuscript.

Code/Data availability

All data are available upon request to the corresponding author.

Competing interests

The authors declare no competing interests.

Acknowledgments

The authors thank the National Natural Science Foundation of China project (42222504) and the Fundamental Research Funds for the Central Universities (14380221, 14380237) for funding.

References

Canagaratna, M. r., Jayne, J. t., Jimenez, J. l., Allan, J. d., Alfarra, M. r., Zhang, Q., Onasch, T. b., Drewnick, F., Coe, H., Middlebrook, A., Delia, A., Williams, L. r., Trimborn, A. m., Northway, M. j., DeCarlo, P. f., Kolb, C. e., Davidovits, P., and Worsnop, D. r.: Chemical and microphysical characterization of ambient aerosols with the aerodyne aerosol mass spectrometer, Mass Spectrometry Reviews, 26, 185–222, https://doi.org/10.1002/mas.20115, 2007.

Canagaratna, M. R., Jimenez, J. L., Kroll, J. H., Chen, Q., Kessler, S. H., Massoli, P., Hildebrandt Ruiz, L., Fortner, E., Williams, L. R., Wilson, K. R., Surratt, J. D., Donahue, N. M., Jayne, J. T., and Worsnop, D. R.: Elemental ratio measurements of organic compounds using aerosol mass spectrometry: Characterization, improved calibration, and implications, Atmospheric Chemistry and Physics, 15, 253–272, https://doi.org/10.5194/acp-15-253-2015, 2015.

Chen, C., Zhang, H., Yan, W., Wu, N., Zhang, Q., and He, K.: Aerosol water content enhancement leads to changes in the major formation mechanisms of nitrate and secondary organic aerosols in winter over the North China Plain, Environmental Pollution, 287, 117625, https://doi.org/10.1016/j.envpol.2021.117625, 2021.

Chen, Q., Miao, R., Geng, G., Shrivastava, M., Dao, X., Xu, B., Sun, J., Zhang, X., Liu,

M., Tang, G., Tang, Q., Hu, H., Huang, R.-J., Wang, H., Zheng, Y., Qin, Y., Guo, S., Hu, M., and Zhu, T.: Widespread 2013-2020 decreases and reduction challenges of organic aerosol in China, Nat Commun, 15, 4465, https://doi.org/10.1038/s41467-024-48902-0, 2024.

Clegg, S. L., Brimblecombe, P., and Wexler, A. S.: Thermodynamic model of the system H^+–NH_4^+–SO_4^{2-}–NO_3^-–H_2O at tropospheric temperatures, J. Phys. Chem. A, 102, 2137–2154, https://doi.org/10.1021/jp973042r, 1998.

DeCarlo, P. F., Kimmel, J. R., Trimborn, A., Northway, M. J., Jayne, J. T., Aiken, A. C., Gonin, M., Fuhrer, K., Horvath, T., Docherty, K. S., Worsnop, D. R., and Jimenez, J. L.: Field-deployable, high-resolution, time-of-flight aerosol mass spectrometer, Anal. Chem., 78, 8281–8289, https://doi.org/10.1021/ac061249n, 2006.

DeCarlo, P. F., Ulbrich, I. M., Crounse, J., de Foy, B., Dunlea, E. J., Aiken, A. C., Knapp, D., Weinheimer, A. J., Campos, T., Wennberg, P. O., and Jimenez, J. L.: Investigation of the sources and processing of organic aerosol over the central mexican plateau from aircraft measurements during MILAGRO, Atmospheric Chemistry and Physics, 10, 5257–5280, https://doi.org/10.5194/acp-10-5257-2010, 2010.

Ding, A., Nie, W., Huang, X., Chi, X., Sun, J., Kerminen, V.-M., Xu, Z., Guo, W., Petäjä, T., Yang, X., Kulmala, M., and Fu, C.: Long-term observation of air pollution-weather/climate interactions at the SORPES station: a review and outlook, Front. Environ. Sci. Eng., 10, 15, https://doi.org/10.1007/s11783-016-0877-3, 2016.

Ding, A., Huang, X., Nie, W., Chi, X., Xu, Z., Zheng, L., Xu, Z., Xie, Y., Qi, X., Shen, Y., Sun, P., Wang, J., Wang, L., Sun, J., Yang, X.-Q., Qin, W., Zhang, X., Cheng, W.,

Liu, W., Pan, L., and Fu, C.: Significant reduction of $PM_{2.5}$ in eastern China due to regional-scale emission control: Evidence from SORPES in 2011–2018, Atmospheric Chemistry and Physics, 19, 11791–11801, https://doi.org/10.5194/acp-19-11791-2019, 2019.

Dou, J., Liu, T., Ge, D., Zhang, Y., Yin, J., Wang, L., Liu, H., Li, D., Niu, G., Chen, L., Wang, J., Qi, X., Nie, W., Chi, X., Huang, X., and Ding, A.: In-situ secondary organic aerosol formation from ambient air in suburban eastern China: Substantially distinct characteristics between summer and winter, Atmospheric Environment, 356, 121295, https://doi.org/10.1016/j.atmosenv.2025.121295, 2025.

Duan, J., Huang, R.-J., Gu, Y., Lin, C., Zhong, H., Xu, W., Liu, Q., You, Y., Ovadnevaite, J., Ceburnis, D., Hoffmann, T., and O'Dowd, C.: Measurement report: Large contribution of biomass burning and aqueous-phase processes to the wintertime secondary organic aerosol formation in Xi'an, Northwest China, Atmos. Chem. Phys., 2022.

Ervens, B., Turpin, B. J., and Weber, R. J.: Secondary organic aerosol formation in cloud droplets and aqueous particles (aqSOA): A review of laboratory, field and model studies, Atmospheric Chemistry and Physics, 11, 11069–11102, https://doi.org/10.5194/acp-11-11069-2011, 2011.

Farmer, D. K., Matsunaga, A., Docherty, K. S., Surratt, J. D., Seinfeld, J. H., Ziemann, P. J., and Jimenez, J. L.: Response of an aerosol mass spectrometer to organonitrates and organosulfates and implications for atmospheric chemistry, Proc. Natl. Acad. Sci. U.S.A., 107, 6670–6675, https://doi.org/10.1073/pnas.0912340107, 2010.

Feng, Z., Liu, Y., Zheng, F., Yan, C., Fu, P., Zhang, Y., Lian, C., Wang, W., Cai, J., Du, W., Chu, B., Wang, Y., Kangasluoma, J., Bianchi, F., Petäjä, T., and Kulmala, M.: Highly oxidized organic aerosols in Beijing: Possible contribution of aqueous-phase chemistry, Atmospheric Environment, 273, 118971, https://doi.org/10.1016/j.atmosenv.2022.118971, 2022.

Freedman, M. A., Ott, E.-J. E., and Marak, K. E.: Role of pH in Aerosol Processes and Measurement Challenges, J. Phys. Chem. A, 123, 1275–1284, https://doi.org/10.1021/acs.jpca.8b10676, 2019.

Gilardoni, S., Massoli, P., Paglione, M., Giulianelli, L., Carbone, C., Rinaldi, M., Decesari, S., Sandrini, S., Costabile, F., Gobbi, G. P., Pietrogrande, M. C., Visentin, M., Scotto, F., Fuzzi, S., and Facchini, M. C.: Direct observation of aqueous secondary organic aerosol from biomass-burning emissions, Proc. Natl. Acad. Sci. U.S.A., 113, 10013–10018, https://doi.org/10.1073/pnas.1602212113, 2016.

Gu, Y., Huang, R.-J., Duan, J., Xu, W., Lin, C., Zhong, H., Wang, Y., Ni, H., Liu, Q., Xu, R., Wang, L., and Li, Y. J.: Multiple pathways for the formation of secondary organic aerosol in the North China Plain in summer, Atmospheric Chemistry and Physics, 23, 5419–5433, https://doi.org/10.5194/acp-23-5419-2023, 2023.

Heald, C. L., Kroll, J. H., Jimenez, J. L., Docherty, K. S., DeCarlo, P. F., Aiken, A. C., Chen, Q., Martin, S. T., Farmer, D. K., and Artaxo, P.: A simplified description of the evolution of organic aerosol composition in the atmosphere, Geophysical Research Letters, 37, https://doi.org/10.1029/2010GL042737, 2010.

Hennigan, C. J., Bergin, M. H., Russell, A. G., Nenes, A., and Weber, R. J.: Gas/particle

451 partitioning of water-soluble organic aerosol in atlanta, Atmospheric Chemistry and
452 Physics, 9, 3613–3628, https://doi.org/10.5194/acp-9-3613-2009, 2009.
453 Hodas, N., Sullivan, A. P., Skog, K., Keutsch, F. N., Decesari, S., Facchini, M. C.,
454 Carlton, A. G., Laaksonen, A., and Turpin, B. J.: Aerosol Liquid Water Driven by
455 Anthropogenic Nitrate: Implications for Lifetimes of Water-Soluble Organic Gases and
456 Potential for Secondary Organic Aerosol Formation, Environ. Sci. Technol., 2014.
457 Huang, R.-J., Zhang, Y., Bozzetti, C., Ho, K.-F., Cao, J.-J., Han, Y., Daellenbach, K. R.,
458 Slowik, J. G., Platt, S. M., Canonaco, F., Zotter, P., Wolf, R., Pieber, S. M., Bruns, E.
459 A., Crippa, M., Ciarelli, G., Piazzalunga, A., Schwikowski, M., Abbaszade, G.,
460 Schnelle-Kreis, J., Zimmermann, R., An, Z., Szidat, S., Baltensperger, U., Haddad, I.
461 E., and Prévôt, A. S. H.: High secondary aerosol contribution to particulate pollution
462 during haze events in China, Nature, 514, 218–222,
463 https://doi.org/10.1038/nature13774, 2014.
464 Huang, R.-J., Li, Y. J., Chen, Q., Zhang, Y., Lin, C., Chan, C. K., Yu, J. Z., de Gouw, J.,
465 Tong, S., Jiang, J., Wang, W., Ding, X., Wang, X., Ge, M., Zhou, W., Worsnop, D., Boy,
466 M., Bilde, M., Dusek, U., Carlton, A. G., Hoffmann, T., McNeill, V. F., and Glasius, M.:
467 Secondary organic aerosol in urban China: A distinct chemical regime for air pollution
468 studies, Science, 389, eadq2840, https://doi.org/10.1126/science.adq2840, 2025.
469 Kanakidou, M., Seinfeld, J. H., Pandis, S. N., Barnes, I., Dentener, F. J., Facchini, M.
470 C., Van Dingenen, R., Ervens, B., Nenes, A., Nielsen, C. J., Swietlicki, E., Putaud, J. P.,
471 Balkanski, Y., Fuzzi, S., Horth, J., Moortgat, G. K., Winterhalter, R., Myhre, C. E. L.,
472 Tsigaridis, K., Vignati, E., Stephanou, E. G., and Wilson, J.: Organic aerosol and global

473 climate modelling: A review, Atmospheric Chemistry and Physics, 5, 1053–1123,
474 https://doi.org/10.5194/acp-5-1053-2005, 2005.
475 Kim, H., Collier, S., Ge, X., Xu, J., Sun, Y., Jiang, W., Wang, Y., Herckes, P., and Zhang,
476 Q.: Chemical processing of water-soluble species and formation of secondary organic
477 aerosol in fogs, Atmospheric Environment, 200, 158–166,
478 https://doi.org/10.1016/j.atmosenv.2018.11.062, 2019.
479 Kuang, Y., He, Y., Xu, W., Yuan, B., Zhang, G., Ma, Z., Wu, C., Wang, C., Wang, S.,
480 Zhang, S., Tao, J., Ma, N., Su, H., Cheng, Y., Shao, M., and Sun, Y.: Photochemical
481 Aqueous-Phase Reactions Induce Rapid Daytime Formation of Oxygenated Organic
482 Aerosol on the North China Plain, Environ. Sci. Technol., 2020.
483 Lim, Y. B., Tan, Y., Perri, M. J., Seitzinger, S. P., and Turpin, B. J.: Aqueous chemistry
484 and its role in secondary organic aerosol (SOA) formation, Atmospheric Chemistry and
485 Physics, 10, 10521–10539, https://doi.org/10.5194/acp-10-10521-2010, 2010.
486 Liu, H., Liu, T., Li, Y., Ge, A., Wang, L., Lai, S., Niu, G., Yin, J., Zhou, X., Liu, Y.,
487 Wang, J., Zha, Q., Qi, X., Nie, W., Chi, X., Lou, S., Huang, X., Zhang, Y., Song, W.,
488 Wang, X., and Ding, A.: Impacts of heatwaves on characteristics of atmospheric
489 methylglyoxal in a suburban area in eastern China, Journal of Geophysical Research:
490 Atmospheres, 130, e2025JD044284, https://doi.org/10.1029/2025JD044284, 2025.
491 Liu, R., Liu, T., Huang, X., Ren, C., Wang, L., Niu, G., Yu, C., Zhang, Y., Wang, J., Qi,
492 X., Nie, W., Chi, X., and Ding, A.: Characteristics and sources of atmospheric ammonia
493 at the SORPES station in the western yangtze river delta of China, Atmospheric
494 Environment, 318, 120234, https://doi.org/10.1016/j.atmosenv.2023.120234, 2024.

Liu, Z., Hu, B., Ji, D., Cheng, M., Gao, W., Shi, S., Xie, Y., Yang, S., Gao, M., Fu, H., Chen, J., and Wang, Y.: Characteristics of fine particle explosive growth events in beijing, China: Seasonal variation, chemical evolution pattern and formation mechanism, Science of The Total Environment, 687, 1073–1086, https://doi.org/10.1016/j.scitotenv.2019.06.068, 2019.

McNeill, V. F.: Aqueous organic chemistry in the atmosphere: Sources and chemical processing of organic aerosols, Environ. Sci. Technol., 49, 1237–1244, https://doi.org/10.1021/es5043707, 2015.

Ng, N. L., Canagaratna, M. R., Jimenez, J. L., Chhabra, P. S., Seinfeld, J. H., and Worsnop, D. R.: Changes in organic aerosol composition with aging inferred from aerosol mass spectra, Atmospheric Chemistry and Physics, 11, 6465–6474, https://doi.org/10.5194/acp-11-6465-2011, 2011.

Nguyen, T. K. V., Zhang, Q., Jimenez, J. L., Pike, M., and Carlton, A. G.: Liquid water: Ubiquitous contributor to aerosol mass, Environ. Sci. Technol. Lett., 3, 257–263, https://doi.org/10.1021/acs.estlett.6b00167, 2016.

Paatero, P. and Tapper, U.: Positive matrix factorization: A non-negative factor model with optimal utilization of error estimates of data values, Environmetrics, 5, 111–126, https://doi.org/10.1002/env.3170050203, 1994.

Peng, J., Hu, M., Shang, D., Wu, Z., Du, Z., Tan, T., Wang, Y., Zhang, F., and Zhang, R.: Explosive secondary aerosol formation during severe haze in the north China plain, Environ. Sci. Technol., 55, 2189–2207, https://doi.org/10.1021/acs.est.0c07204, 2021.

Pye, H. O. T., Nenes, A., Alexander, B., Ault, A. P., Barth, M. C., Clegg, S. L., Collett

517 Jr., J. L., Fahey, K. M., Hennigan, C. J., Herrmann, H., Kanakidou, M., Kelly, J. T., Ku,
518 I.-T., McNeill, V. F., Riemer, N., Schaefer, T., Shi, G., Tilgner, A., Walker, J. T., Wang,
519 T., Weber, R., Xing, J., Zaveri, R. A., and Zuend, A.: The acidity of atmospheric
520 particles and clouds, Atmospheric Chemistry and Physics, 20, 4809–4888,
521 https://doi.org/10.5194/acp-20-4809-2020, 2020.
522 Rogers, M. J., Joo, T., Hass-Mitchell, T., Canagaratna, M. R., Campuzano-Jost, P.,
523 Sueper, D., Tran, M. N., Machesky, J. E., Roscioli, J. R., Jimenez, J. L., Krechmer, J.
524 E., Lambe, A. T., Nault, B. A., and Gentner, D. R.: Humid summers promote urban
525 aqueous-phase production of oxygenated organic aerosol in the northeastern united
526 states, Geophysical Research Letters, 52, e2024GL112005,
527 https://doi.org/10.1029/2024GL112005, 2025.
528 Seinfeld, J. H. and Pankow, J. F.: Organic atmospheric particulate material, Annu. Rev.
529 Phys. Chem., 54, 121–140,
530 https://doi.org/10.1146/annurev.physchem.54.011002.103756, 2003.
531 Sullivan, A. P., Hodas, N., Turpin, B. J., Skog, K., Keutsch, F. N., Gilardoni, S.,
532 Paglione, M., Rinaldi, M., Decesari, S., Facchini, M. C., Poulain, L., Herrmann, H.,
533 Wiedensohler, A., Nemitz, E., Twigg, M. M., and Collett Jr., J. L.: Evidence for ambient
534 dark aqueous SOA formation in the Po Valley, Italy, Atmos. Chem. Phys., 16, 8095–
535 8108, https://doi.org/10.5194/acp-16-8095-2016, 2016.
536 Sun, P., Nie, W., Chi, X., Xie, Y., Huang, X., Xu, Z., Qi, X., Xu, Z., Wang, L., Wang,
537 T., Zhang, Q., and Ding, A.: Two years of online measurement of fine particulate nitrate
538 in the western Yangtze River Delta: influences of thermodynamics and N_2O_5 hydrolysis,

Atmos. Chem. Phys., 18, 17177–17190, https://doi.org/10.5194/acp-18-17177-2018, 2018.

Sun, W., Wang, D., Yao, L., Fu, H., Fu, Q., Wang, H., Li, Q., Wang, L., Yang, X., Xian, A., Wang, G., Xiao, H., and Chen, J.: Chemistry-triggered events of $PM_{2.5}$ explosive growth during late autumn and winter in shanghai, China, Environmental Pollution, 254, 112864, https://doi.org/10.1016/j.envpol.2019.07.032, 2019.

Sun, Y., Du, W., Fu, P., Wang, Q., Li, J., Ge, X., Zhang, Q., Zhu, C., Ren, L., Xu, W., Zhao, J., Han, T., Worsnop, D. R., and Wang, Z.: Primary and secondary aerosols in Beijing in winter: sources, variations and processes, Atmospheric Chemistry and Physics, 16, 8309–8329, https://doi.org/10.5194/acp-16-8309-2016, 2016.

Sun, Y. L., Zhang, Q., Anastasio, C., and Sun, J.: Insights into secondary organic aerosol formed via aqueous-phase reactions of phenolic compounds based on high resolution mass spectrometry, Atmospheric Chemistry and Physics, 10, 4809–4822, https://doi.org/10.5194/acp-10-4809-2010, 2010.

Tilgner, A., Schaefer, T., Alexander, B., Barth, M., Collett Jr., J. L., Fahey, K. M., Nenes, A., Pye, H. O. T., Herrmann, H., and McNeill, V. F.: Acidity and the multiphase chemistry of atmospheric aqueous particles and clouds, Atmos. Chem. Phys., 21, 13483–13536, https://doi.org/10.5194/acp-21-13483-2021, 2021.

Ulbrich, I. M., Canagaratna, M. R., Zhang, Q., Worsnop, D. R., and Jimenez, J. L.: Interpretation of organic components from Positive Matrix Factorization of aerosol mass spectrometric data, Atmos. Chem. Phys., 2009.

Wang, F., Lv, S., Liu, X., Lei, Y., Wu, C., Chen, Y., Zhang, F., and Wang, G.:

Investigation into the differences and relationships between gasSOA and aqSOA in winter haze pollution on Chongming Island, Shanghai, based on VOCs observation, Environmental Pollution, 316, 120684, https://doi.org/10.1016/j.envpol.2022.120684, 2023.

Wang, J., Ge, X., Chen, Y., Shen, Y., Zhang, Q., Sun, Y., Xu, J., Ge, S., Yu, H., and Chen, M.: Highly time-resolved urban aerosol characteristics during springtime in yangtze river delta, China: Insights from soot particle aerosol mass spectrometry, Atmospheric Chemistry and Physics, 16, 9109–9127, https://doi.org/10.5194/acp-16-9109-2016, 2016.

Wang, J., Ye, J., Zhang, Q., Zhao, J., Wu, Y., Li, J., Liu, D., Li, W., Zhang, Y., Wu, C., Xie, C., Qin, Y., Lei, Y., Huang, X., Guo, J., Liu, P., Fu, P., Li, Y., Lee, H. C., Choi, H., Zhang, J., Liao, H., Chen, M., Sun, Y., Ge, X., Martin, S. T., and Jacob, D. J.: Aqueous production of secondary organic aerosol from fossil-fuel emissions in winter Beijing haze, Proc. Natl. Acad. Sci. U.S.A., 118, e2022179118, https://doi.org/10.1073/pnas.2022179118, 2021.

Wexler, A. S. and Clegg, S. L.: Atmospheric aerosol models for systems including the ions H^+, NH_4^+, Na^+, SO_4^{2-}, NO_3^-, Cl^-, Br^-, and H_2O, Journal of Geophysical Research: Atmospheres, 107, ACH 14-1-ACH 14-14, https://doi.org/10.1029/2001JD000451, 2002.

Wu, Y., Ge, X., Wang, J., Shen, Y., Ye, Z., Ge, S., Wu, Y., Yu, H., and Chen, M.: Responses of secondary aerosols to relative humidity and photochemical activities in an industrialized environment during late winter, Atmospheric Environment, 193, 66–

78, https://doi.org/10.1016/j.atmosenv.2018.09.008, 2018.

Xian, J., Cui, S., Chen, X., Wang, J., Xiong, Y., Gu, C., Wang, Y., Zhang, Y., Li, H., Wang, J., and Ge, X.: Online chemical characterization of atmospheric fine secondary aerosols and organic nitrates in summer Nanjing, China, Atmospheric Research, 290, 106783, https://doi.org/10.1016/j.atmosres.2023.106783, 2023.

Xiao, Y., Hu, M., Li, X., Zong, T., Xu, N., Hu, S., Zeng, L., Chen, S., Song, Y., Guo, S., and Wu, Z.: Aqueous secondary organic aerosol formation attributed to phenols from biomass burning, Science of The Total Environment, 847, 157582, https://doi.org/10.1016/j.scitotenv.2022.157582, 2022.

Xu, W., Han, T., Du, W., Wang, Q., Chen, C., Zhao, J., Zhang, Y., Li, J., Fu, P., Wang, Z., Worsnop, D. R., and Sun, Y.: Effects of Aqueous-Phase and Photochemical Processing on Secondary Organic Aerosol Formation and Evolution in Beijing, China, Environ. Sci. Technol., 51, 762–770, https://doi.org/10.1021/acs.est.6b04498, 2017.

Xu, W., Sun, Y., Wang, Q., Zhao, J., Wang, J., Ge, X., Xie, C., Zhou, W., Du, W., Li, J., Fu, P., Wang, Z., Worsnop, D. R., and Coe, H.: Changes in Aerosol Chemistry From 2014 to 2016 in Winter in Beijing: Insights From High-Resolution Aerosol Mass Spectrometry, Journal of Geophysical Research: Atmospheres, 124, 1132–1147, https://doi.org/10.1029/2018JD029245, 2019.

Yasmeen, F., Sauret, N., Gal, J.-F., Maria, P.-C., Massi, L., Maenhaut, W., and Claeys, M.: Characterization of oligomers from methylglyoxal under dark conditions: A pathway to produce secondary organic aerosol through cloud processing during nighttime, Atmospheric Chemistry and Physics, 10, 3803–3812,

https://doi.org/10.5194/acp-10-3803-2010, 2010.

Zhao, J., Qiu, Y., Zhou, W., Xu, W., Wang, J., Zhang, Y., Li, L., Xie, C., Wang, Q., Du, W., Worsnop, D. R., Canagaratna, M. R., Zhou, L., Ge, X., Fu, P., Li, J., Wang, Z., Donahue, N. M., and Sun, Y.: Organic Aerosol Processing During Winter Severe Haze Episodes in Beijing, JGR Atmospheres, 124, 10248–10263, https://doi.org/10.1029/2019JD030832, 2019.

Zhou, J., Elser, M., Huang, R.-J., Krapf, M., Fröhlich, R., Bhattu, D., Stefenelli, G., Zotter, P., Bruns, E. A., Pieber, S. M., Ni, H., Wang, Q., Wang, Y., Zhou, Y., Chen, C., Xiao, M., Slowik, J. G., Brown, S., Cassagnes, L.-E., Daellenbach, K. R., Nussbaumer, T., Geiser, M., Prévôt, A. S. H., El-Haddad, I., Cao, J., Baltensperger, U., and Dommen, J.: Predominance of secondary organic aerosol to particle-bound reactive oxygen species activity in fine ambient aerosol, Atmospheric Chemistry and Physics, 19, 14703–14720, https://doi.org/10.5194/acp-19-14703-2019, 2019.

Ziemann, P. J. and Atkinson, R.: Kinetics, products, and mechanisms of secondary organic aerosol formation, Chem. Soc. Rev., 41, 6582–6605, https://doi.org/10.1039/C2CS35122F, 2012.